Journal of Materials Processing Technology 236 (2016) 183–188

Contents lists available at ScienceDirect

Journal of Materials Processing Technology

journal homepage: www.elsevier.com/locate/jmatprotec

Micro-ultrasonic welding using thermoplastic-elastomeric composite film

Wei Xuan Chan[a,b], Sum Huan Ng[b], King Ho Holden Li[a], Woo-Tae Park[c], Yong-Jin Yoon[a,*]

[a] School of Mechanical and Aerospace Engineering, Nanyang Technological University, 50 Nanyang Avenue, S 639798, Singapore
[b] Singapore Institute of Manufacturing Technology, 71 Nanyang Dr, Singapore 638075, Singapore
[c] Department of Mechanical and Automotive Engineering, Seoul National University of Science and Technology, Gongreung-2 dong, Nowon-gu, Seoul 139-743, South Korea

ARTICLE INFO

Article history:
Received 11 March 2016
Received in revised form 20 May 2016
Accepted 21 May 2016
Available online 24 May 2016

Keywords:
Ultrasonic welding
PMMA
PDMS
Microfluidics
Composite

ABSTRACT

A composite film of PMMA microspheres in PDMS is used as the fusion layer to avoid trapped air and to restrict the flow of the melted polymer during welding. The matrix material selection and distribution of PMMA microspheres is determined by the 1-D theoretical model. The theoretical work reveals that the difference in dynamic modulus between the matrix material and PMMA is the most significant contribution to the viability of this composite ultrasonic welding film. The experiment is conducted with PDMS as the matrix material to determine effect of the concentration of PMMA microspheres as micro energy directors on the welding strength and quality of the proposed methodology with the chosen composite. While there are no visible signs of trapped air in all specimens, the resultant welding strength in this methodology is limited by the particle size range of the PMMA microspheres. For ultrasonic energy input of 1 kJ on a 32 mm × 32 mm sample, the optimum concentration of PMMA microspheres is found to be 0.24.

1. Introduction

Recently, there has been tremendous interest in microfludics for applications in biomedical due to their ability to provide fast response and low cost production with only trace amounts of chemical bio-receptors. The microfluidic devices are usually fabricated using glass or silicon with chemical and plasma etching, and photolithography. Becker and Locascio (2002) reviewed other materials including polymethyl methacrylate (PMMA) and polydimethylsiloxane (PDMS) which are commonly preferred in industries as cheaper alternatives to glass. Kalkandjiev et al. (2011) highlighted the low fabrication cost and the ease to mass produce as the major reasons of using PDMS and PMMA, and Luo et al. (2010) demonstrated that the PMMA also have the potential to create complex, stable geometries using simple fabrication methods (without fabricating energy directors), while being able to accommodate errors in terms of reversible change upon softening and melting.

In the production of microfluidic devices, Luo et al. (2010) highlighted the critical role of the welding process in sealing open microstructures and allowing integration into a closed fluidic paths. There are numerous welding techniques including capillary adhesive welding, chamber adhesive welding, adhesive film welding, laser welding, solvent diffusion welding, conventional thermal welding and plasma assisted (thermal) welding. There are also techniques such as UV degradation supported thermal welding, developed by Truckenmuller et al. (2006), which applies to a few types of polymers only. The main welding research on these techniques focused on finding the ideal process that has short process time and retains the channel geometrical structure while still produces high strength welds. However, there are not much breakthroughs in the efficiency of mass production of microfluidic devices due to welding process time and weld quality of existing techniques. The stability of design geometry and strength of welding are important criterion the manufacturing of microfluidic devices. Hence, Zhang et al. (2010b) provided guidelines that the welding has to be tight sealing at joint interface and void of contaminants. They (Zhang et al., 2010a) also added that the process has to create minimal deformation of the existing microstructures.

Ultrasonic welding is a technique in which the specimens are connected by the melting of plastic with ultrasonic acoustic energy source. Benatar and Gutowski (1989) claimed the high efficiency of this method due to its stability and ability to produce strong joints with automated compact equipment, and Ng et al. (2009) use ultrasonic welding to join connectors which enables rapid process time (in the order of seconds) and economical mass production

* Corresponding author.
E-mail address: yongjiny@ntu.edu.sg (Y.-J. Yoon).

http://dx.doi.org/10.1016/j.jmatprotec.2016.05.025
0924-0136/

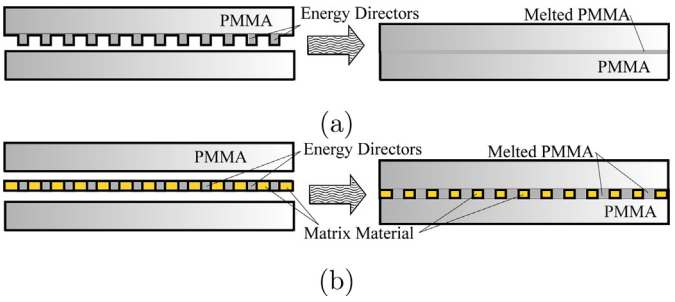

Fig. 1. Illustration of polymer using (a) conventional and (b) composite film ultrasonic welding. In conventional ultrasonic welding, the energy directors melt and flow across the surface of the samples, resulting in a thinner fusion layer. In ultrasonic welding using composite film, the energy directors melts but maintains its height due flow restriction by the matrix material.

of the microfluidic devices. Rani et al. (2007) studied the parameters in ultrasonic welding and gave an better understanding to the process. The ultrasonic welding process, with current simplicity of operation developed by Grewell (1999), utilizes an ultrasonic energy source (usually with a frequency of 20–50 kHz) and low amplitude (15–60 μm) mechanical vibration to induce localized frictional heating through viscoelastic dissipation by intermolecular friction. The generated heat melts contacting surfaces of the polymer and joins the two surfaces.

Truckenmuller et al. (2006) fabricated the first ultrasonically welded microfluidic device by concentrating energy with convex energy directors. The time for energy director to melt is in the order of seconds. Therefore, it is difficult to precisely control the flow of the melted polymer. Although, overflow and underflow of molten polymer is acceptable for welding of most macro devices, Zhang et al. (2010b) have highlighted that it may clog (overflow) or leave small gaps (underflow) in the micro structures and cause a microfluidic device to be unusable. Sun et al. (2012) used micro energy directors to allow more space for the flow of molten PMMA. However, this does not eliminate problems of overflow and underflow entirely and it also causes air trapped when the energy directors are tightly arranged.

This present study explores the feasibility of using a composite film made of distributed thermoplastic particles in an elastomeric matrix to restrict the flow of melted energy directors and eliminate problems of trapped air, thus reducing its impact on the shapes of flow channels of microfluidic devices. The design process includes the matrix material selection, energy director distribution and optimizing the ultrasonic welding process parameters. Experiments are also conducted on the welding strength of PMMA samples welded using the present methodology.

2. Method

The fusion layer of the ultrasonic process in this work is a thin composite film consisting of micro-energy directors and a elastomeric matrix. The elastomeric matrix would constrict the flow of PMMA energy directors when they are in viscous state as well as replace the air which might be otherwise trapped during the process. Fig. 1 shows the ultrasonic welding using air (conventional) and elastomeric polymer as matrix. Other than the presence of trapped air and uncontrolled molten polymer flow, the two main notable differences of the welded products are the change in separation distance (shown in Fig. 1) and welding strength. The change in separation distance of conventional ultrasonic welding is,

$$h_s = h_{ed} - \frac{Vol_{ed}}{A} \tag{1}$$

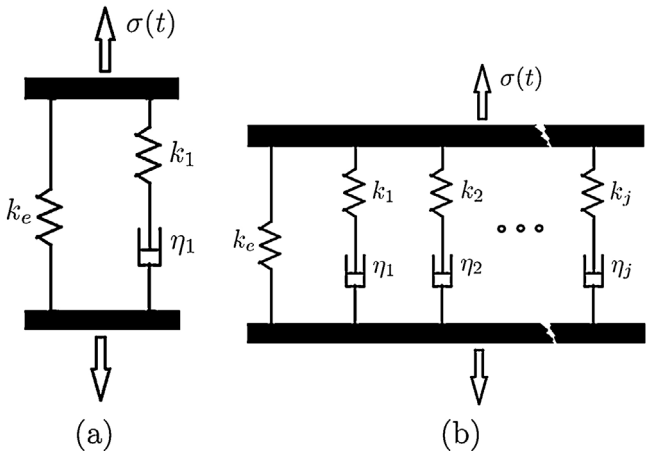

Fig. 2. (a) Maxwell standard linear solid and (b) Wiechert model (Wineman and Rajagopal, 2000). The viscoelastic materials of the thermoplastic-elastomeric composite is modeled as a system of springs and Newton dashpots. In a small range of temperature and vibration frequency, we approximate the Wiechert model to the Maxwell standard linear solid with equivalent spring and damping constants.

where h_{ed} is the initial height of the energy directors, Vol_{ed} is the total volume of the energy directors and A is the area of material welding (excluding channels, etc.). The change in separation distance using composite film is negligible due to incompressibility of the matrix material.

In this section, a methodology of composite material selection and design with a theoretical model for initial feasibility analysis followed by an experimental verification of such design is presented. The 1-dimensional theoretical model assesses the suitability of different matrix material as well as distribution of energy directors on the composite welding film. For this work, PDMS is chosen as the matrix material based on studies from the theoretical model after comparing some common elastomeric materials. The composite is fabricated by spin coating PMMA-microspheres-mixed-PDMS-base. Following so, the experiment presents the effect of different composite ratio on the welding strength of the proposed method. The experimental result also elucidates limitation of the fabrication method.

2.1. Ultrasonic welding model

Benatar and Gutowski (1989) categorized the mechanism of ultrasonic welding into mechanics and vibrations, viscoelastic heating of thermoplastic, heat transfer process, flow and wetting, and intermolecular diffusion. In this model, the mechanics and viscoelastic heating of thermoplastic is considered for the purpose of material choosing and energy director distribution. The Maxwell form of the standard linear solid (SLS) (Fig. 2(a)) is adopted to estimate the strain response with material parameters.

The strain response for input stress, $\sigma(t) = \sigma_0 \cos(\omega t) + \sigma_c$, in SLS is,

$$\epsilon(t) = \sigma_0 R \cos(\omega t - \delta) + \frac{\sigma_c}{k_e + k_1} \tag{2}$$

$$R^2 = U^2 + V^2 \tag{3}$$

$$U = \frac{(k_e + k_1)^2(\tau\omega)^2 + k_e^2 + k_1 k_e}{(k_e + k_1)[(k_e + k_1)^2(\tau\omega)^2 + k_e^2]} \tag{4}$$

$$V = \frac{k_1(k_e + k_1)(\tau\omega)}{(k_e + k_1)[(k_e + k_1)^2(\tau\omega)^2 + k_e^2]} \tag{5}$$

$$\delta = \tan^{-1}\frac{V}{U} \tag{6}$$

where $\tau_i = \eta_i / k_i$.

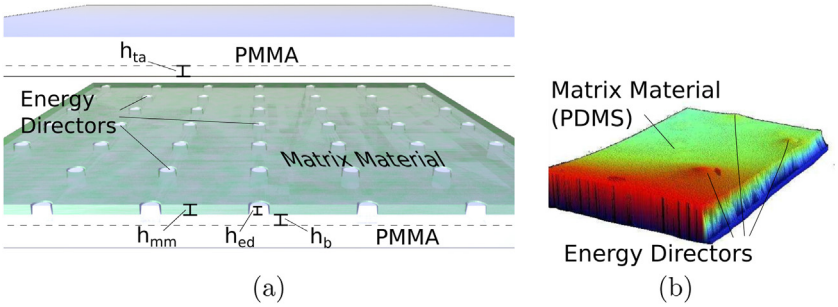

Fig. 3. Design of composite film to prevent overflow of PMMA during ultrasonic welding. (a) Cross-section of the composite model where h_b and h_{ta} are the effective height of the base PMMA and target PMMA respectively. h_{ed} and h_{mm} are the height of the PMMA energy directors and matrix material thickness respectively. (b) White light interferometry analysis of the PMMA-microspheres-mixed-PDMS composite on a PMMA substrate.

Due to the time scale difference in the ultrasonic frequency and change in temperature, a constant temperature is assumed within one cycle of oscillation and the averaged net power dissipation per volume (PDPV) is,

$$P = \frac{\sigma_0^2 \omega}{2} V \tag{7}$$

During ultrasonic welding, the total changes in length of the sample at areas with the energy directors and with the matrix material are,

$$L_{ed}(t) = \epsilon_b(t)h_b + \epsilon_{ta}(t)h_{ta} + \epsilon_{ed}(t)h_{ed} - (h_{mm} - h_{ed}) \tag{8}$$

$$L_{mm}(t) = \epsilon_b(t)h_b + \epsilon_{ta}(t)h_{ta} + \epsilon_{mm}(t)h_{mm} \tag{9}$$

where Fig. 3(a) shows the denotations of the equation, and h_b and h_{ta} are the effective length due to the non-uniformity and coarse distribution of the energy directors where beyond the effective length, there is an uniform distribution of stress. The effective length also depends on the stiffness of the PMMA and matrix material.

Considering the balance of force and comparing the time varying component of $L_{mm}(t) = L_{ed}(t)$, the ratio of PDPV (from Eq. (7)), α, is,

$$\left(\frac{P_{PMMAed}}{P_{PMMAmm}}\right) = \frac{(h_{efr})^2 + R_m^2\left(\frac{h_{mm}}{h_{ed}}\right)^2 + 2R_m R_d \cos(\delta_M) h_{efr}\frac{h_{mm}}{h_{ed}}}{\frac{\sin(\delta_{PMMAmm})}{\sin(\delta_{PMMAed})} R_d[(h_{efr})^2 + 1 + 2h_{efr}]} \tag{10}$$

where $h_{efr} = (h_b + h_{ta})/h_{ed}$, $R_d = R_{PMMAmm}/R_{PMMAed}$, $R_m = R_{MM}/R_{PMMAmm}$ and $\delta_M = \delta_{PMMAmm} - \delta_{MM}$. The subscripts 'MM' and 'PMMA' denotes the matrix and PMMA materials respectively, and the subscripts 'mm' and 'ed' denotes the area with PMMA-matrix material and PMMA-PMMA contact respectively.

The power dissipation in the energy director as a ratio of the total power dissipation is,

$$\left(\frac{Power_{PMMAed}}{Power_{Total}}\right) = \frac{\alpha A_r}{\alpha A_r(1 + h_{efr}) + (h_{efr}) + \frac{V_{MM}}{V_{PMMAmm}}\left(\frac{h_{mm}}{h_{ed}}\right)} \tag{11}$$

where $A_r = A_{ed}/A_{mm}$.

2.1.1. Effect of matrix material properties and distribution of energy directors

The terms in the numerator and denominator in Eq. (10) are compared to determine the significant factors affecting the PDPV ratio. The ratio of sine terms and the term R_d in the denominator represent the contribution of the change of PMMA's viscoelastic damping and dynamic modulus with temperature on the PDPV ratio.

Considering the small differences in other factors, $R_m(h_{mm}/h_{ed})$ is the determining factor on the feasibility of using any material as the matrix. Matrix material selection has to satisfy the condition, $min(R_{MM})h_{mm} > R_{PMMA}h_{ed}$ to ensure that the PDPV is always greater at the energy directors contact area regardless of the temperature of the matrix material. The effective length ratio in the first term reduces the effect of R_m in the PDPV ratio.

The third term indicates that the ratio of PDPV at energy director contact area reduces with the increased difference between the viscoelasticity of the materials ($\delta_{PMMA} - \delta_{MM}$) and the extent of the effect is determined by the effective length ratio, $(h_b + h_{ta})/h_{ed}$. This particular conclusion corroborates with the experiment by Sun et al. (2012) (Fig. 8(a)) where widening the dimension of the energy directors (making the distribution coarser) reduces the percentage area of fusion.

2.1.2. Composite material selection and design

In actual materials, the Wiechert model (Fig. 2(b)) represents the dynamics of the viscoelasticity more closely than the SLS model (Fig. 2(a)). We can reduce the Wiechert model to the SLS model with equivalent k_e and k_1 where the viscoelastic effect is the greatest ($\delta V/\delta(\tau\omega) = 0$) by grouping together relaxation time, τ_i, of the same order.

Capodagli and Lakes (2008) concluded that Arrhenius form is more accurate in predicting the temperature shift in PMMA,

$$\frac{\tau(T)}{\tau(T_{ref})} = e^{\Delta H/R((1/T)-(1/T_{ref}))} \tag{12}$$

where ΔH is the activation energy of mechanism of internal friction taken to be 7.1 kJ/mol (McCrum et al., 1997) and R is the gas constant. With this estimations, we obtain the properties graph $1/R[\tau(T), \omega_{ref}]$ (Fig. 4(a)) from Lee et al.'s (2000) measurements of dynamic modulus in the frequency domain.

Capodagli and Lakes (2008) measures the changes in the inverse damping peak of PMMA experimentally and approximate it to,

$$\frac{1}{\tan\delta_{peak}} = -0.1108(T - 273.15) + 17.410 \tag{13}$$

where T is the temperature in Kelvin and the damping, $\tan\delta_{peak}$, approaches infinity at melting temperature of PMMA. This property of PMMA, together with Eq. (10), reveals two mechanism in the ultrasonic welding of PMMA. At the start where temperatures are similar, the concentration of energy is achieved by the term $R_m(h_{mm}/h_{ed})$. When the temperatures difference increases, the PDPV ratio increase exponentially due to the increase damping of PMMA (ratio of sine terms in Eq. (10)).

PDMS is an excellent choice for matrix material for PMMA with its R value approximately 2 orders higher than PMMA (Fig. 4(a)). With such large value R_m, the PDPV ratio can be approximate to R_m^2. Although, the difference in damping, V/U, of PMMA and PDMS is relatively large compared to other polymers (Fig. 4(b)), the value of cosine term in Eq. (10) varies between 0.95 and 1 only.

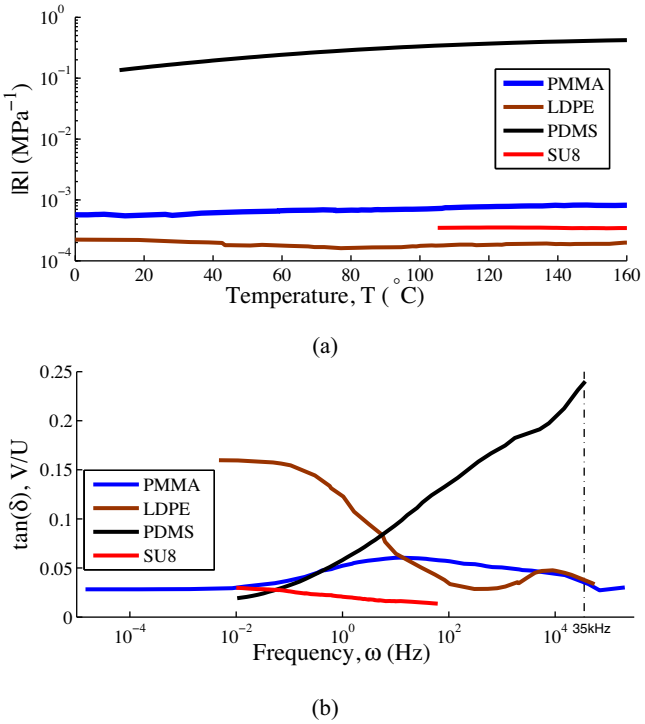

Fig. 4. (a) Inverse dynamic modulus, $|R|$, and (b) damping, $\tan\delta = V/U$ of PMMA and LDPE (Lee et al., 2000) using broadband viscoelasticity spectrometer, a method developed by Brodt et al. (1995), as well as 3–4 mm PDMS and 0.13 mm SU8 (Le Rouzic et al., 2009) using a commercial BOSE Electroforce 3200 machine. Measurements at temperature, $T = 23\,^{\circ}C$. The temperature-time shift is approximated with Arrhenius form.

2.2. Experiment

2.2.1. Preparation of composite film

PMMA microspheres with a variance over mean diameter ratio of 0.34 and 0.32 is used in conduction with PDMS to study its effect on welding and controlled melting. The use of PMMA microspheres enables slightly non-uniform distribution to show a minimal bonding strength in the experiment so that the conditions would be closer to practical microfluidic devices with multiple channels. It also shows the possibility for future fabrications of ready-to-use composite films for ultrasonic welding. Using an optical microscope, we found that the PMMA microspheres had a distribution mean of 260.2 μm by 271.8 μm and variance of 88.6 μm and 87.2 μm respectively. We introduced the PMMA microspheres with precise concentration into a PDMS mixture of a fixed recipe of 184 silicone elastomer base and curing agent at a ratio of 10:1, spin coated the mixture onto a PMMA substrate and cured it at 80 °C for 30 min. We established that spin coating parameters of 1000 rpm for 30 s (Fig. 5) provides the best control over the distribution of PMMA microspheres.

2.2.2. Ultrasonic welding process and pull test

We welded the PMMA welding plate (32 mm × 32 mm) to a blank PMMA base plate (40 mm × 40 mm) using the Hermann Ultrasonic Welding Machine with base fixture and platform leveled to ensure balanced and equal welding across the welding plate. The frequency, maximum power, weld force and displacement amplitude were 35 kHz, 1 kW, 100 N and 16.25 μm respectively. We set the trigger height at values between 15–20 μm and adjusted the ultrasonic horn to control to trigger height within the trigger window.

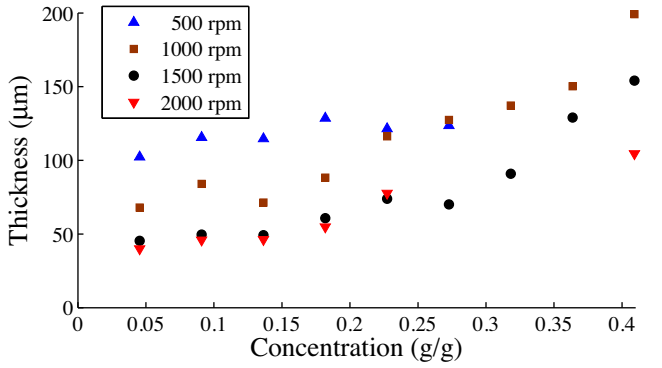

Fig. 5. PDMS spin coated thickness with different rotating speed and PMMA microspheres concentration. The error of the thickness value to any trend is caused by the large variance of the PMMA microspheres size.

Two settings were used in the experiment. The optimal parameters (welding time of 1.5 s) is reference from results on non-coated PMMA with energy director hot embossed onto the plate surface. We also used alternative parameters which reduces the welding time to 1 s to prevent over-welding as there are high amount of melt and shattering present in samples welded with optimum parameters (Fig. 6(a)). This pattern of melt could be caused partially by the difference in sizes of the PMMA powder. Since ultrasonic welding at such a micro level requires precision leveling, these deviation in sizes present a certain level of difficulty in obtaining a good weld. However, in the adapted parameters which the weld time is 1s, the resulting weld produced a much better weld (Fig. 6(b)).

Welding strength is determined by a tensile pull test using the Instron Microtester. Pull test to break is executed at a rate of 5 mm/min after calibrating the tester with fine positioning, load balancing and gauge length zeroing.

3. Results and discussions

For the alternative parameters, the concentration of 0.24 is optimum where the energy input is able to melt all the PMMA microspheres. Any further increase in concentration of PMMA microspheres requires a longer welding time. However, with a longer welding time (such as that of the optimum parameters), Fig. 1(a) shows undesirable over-welding at the edge on one side of the samples. This over welding is due to the diverse distribution of the PMMA microspheres diameter, which cause PDMS mixture coating to be highly non-level at high concentrations of PMMA microspheres. The overwelding can also be seen from the optimum parameters trend line which is much higher than that of the alternative parameters and the model's estimates of optimum parameters, and it does not appear to have any maximum at any concentration of PMMA microspheres (Fig. 7).

While there are no visible signs of overflow, underflow and trapped air in all specimens, the resultant welding strength in this methodology is limited by the particle size range of the PMMA microspheres. Composite with larger range of microspheres size has a lower maximum ultrasonic energy which it can be subjected to before over melting occurs. This limits the maximum welding strength at ≈35 kPa (Fig. 7) for composite film with concentration of 0.24. Reducing the variance of the PMMA microsphere diameter distribution would allow increased welding time without risk of over-welding. The local welding strength, σ_{LWS}, can be approximated with Fig. 7,

$$\sigma_{LWS} \approx \frac{d\sigma_T}{dc} \times \frac{\rho_{PMMA}}{\rho_{PDMS}} \tag{14}$$

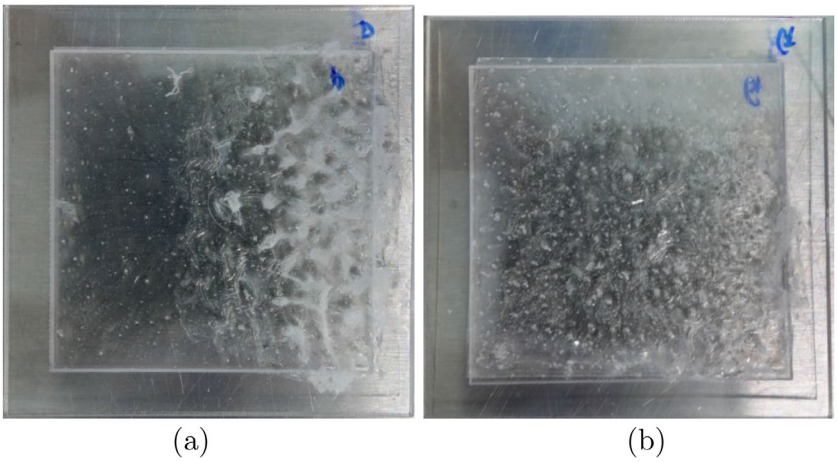

Fig. 6. Ultrasonic welding of composite film coated PMMA samples with (a) 100% amplitude (1 kW), 100 N weld force, 1.5 s weld time (optimum parameters) and (b) 100% amplitude (1 kW), 100 N weld force, 1 s weld time (adapted parameters).

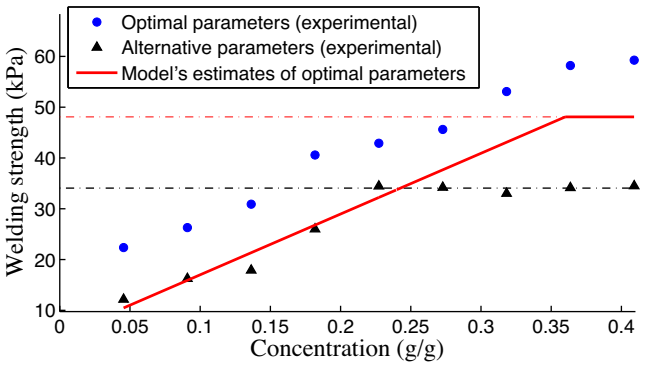

Fig. 7. PMMA plate welding strength with spin coated PDMS with PMMA microspheres mixture at different concentrations (mass of PMMA microspheres/total mass of PDMS with curing agent). The model's (Eq. (15)) estimates of optimum parameters curve (without over-welding) from alternative parameters curve is also plotted. The horizontal lines depict the limit of welding strength of the samples with the respective ultrasonic welding parameters.

where σ_T is the total welding strength of the sample. The local welding strength is approximated to be 188 kPa.

With matrix material of large α wrt PMMA such as PDMS, the total power dissipation ratio (Eq. (11)) can be approximated to $1/(1+h_{efr})$ = constant, which is similar to a fusion layer without the matrix material in Sun et al.'s (2012) micro energy directors. This effect of a constant total power dissipation ratio regardless of energy director height and concentration can be seen from the straight line trend of the alternative parameters in Fig. 7. Taking reference from the experimental results of the alternative parameters, the energy input required can be calculated,

$$E = 1.53 \times 10^{10} cAh \quad (15)$$

where E is the energy input, c is the PMMA microsphere concentration, A is the area of the sample and h is the mean diameter of the PMMA microspheres (all parameters in SI unit).

4. Conclusions

The matrix material selection is significantly determined by the ratio of dynamic modulus of the matrix material over that of the PMMA. The welding strength of the PDMS-PMMA microspheres (with a variance over mean diameter ratio of ≈0.33) composite film is up to 35 kPa at a concentration of 0.24. The proposed methodology of ultrasonic welding provides an option to compromise welding strength for better control of molten polymer flow and problems of trapped air in welded samples.

Acknowledgements

This work was funded by School of Mechanical and Aerospace Engineering, Nanyang Technological University, MOE AcRF Tier 1 (RG 93/13, RG 35/12, and RG C4/13) and the Singapore Institute of Manufacturing Technology (SIMTech), under the Agency for Science, Technology and Research (A*STAR, Singapore). This work was also supported by the Radiation Technology R&D program through the National Research Foundation of Korea funded by the Ministry of Science, ICT & Future Planning (NRF-2013M2A2A9043274).

References

Becker, H., Locascio, L.E., 2002. Polymer microfluidic devices. Talanta 56 (2), 267, ISSN 00399140.
Benatar, A., Gutowski, T.G., 1989. Ultrasonic welding of peek graphite APC-2 composites. Polym. Eng. Sci. 29 (23), 1705–1721.
Brodt, M., Cook, L.S., Lakes, R.S., 1995. Apparatus for measuring viscoelastic properties over ten decades: refinements. Rev. Sci. Instrum. 66 (11), 5292–5297, http://dx.doi.org/10.1063/1.1146101, ISSN 0034-6748.
Capodagli, J., Lakes, R., 2008, September. Isothermal viscoelastic properties of PMMA and LDPE over 11 decades of frequency and time: a test of time-temperature superposition. Rheol. Acta 47 (7), 777–786, http://dx.doi.org/10.1007/s00397-008-0287-y, ISSN 0035-4511.
Grewell, D.A., 1999. A prototype 'expert' system for ultrasonic welding of plastics. Plast. Eng. 33 (2), ISSN 0091-9578.
Kalkandjiev, K., Riegger, L., Kosse, D., Welsche, M., Gutzweiler, L., Zengerle, R., Koltay, P., 2011. Microfluidics in silicon/polymer technology as a cost-efficient alternative to silicon/glass. J. Micromech. Microeng. 2 (2).
Le Rouzic, J., Delobelle, P., Vairac, P., Cretin, B., 2009. Comparison of three different scales techniques for the dynamic mechanical characterization of two polymers (PDMS and SU8). Eur. Phys. J. - Appl. Phys. 48 (01), 1–14, http://dx.doi.org/10.1051/epjap/2009124, ISSN 1286-0050.
Lee, T., Lakes, R.S., Lal, A., 2000. Resonant ultrasound spectroscopy for measurement of mechanical damping: comparison with broadband viscoelastic spectroscopy. Rev. Sci. Instrum. 71 (7), 2855–2861, http://dx.doi.org/10.1063/1.1150703.
Luo, Y., Zhang, Z.B., Wang, X.D., Zheng, Y.S., 2010. Ultrasonic bonding for thermoplastic microfluidic devices without energy director. Microelectron. Eng. Anal. Bound. Elem. 87 (11), ISSN 11.
McCrum, N., Buckley, C., Bucknall, C., 1997. Principles of Polymer Engineering, 2nd ed. Oxford University Press, ISBN 978-0-19-856526-0.
Ng, S.H., Wang, Z.F., de Rooij, N.F., 2009. Microfluidic connectors by ultrasonic welding. Microelectron. Eng. 86 (4-6), 1354–1357, http://dx.doi.org/10.1016/j.mee.2009.01.048, ISSN 01679317.
Rani, R.M., Suresh, K.S., Prakasan, K., Rudramoorthy, R., 2007. A statistical study of parameters in ultrasonic welding of plastics. Exp Tech. 53 (5), http://dx.doi.org/10.1111/j.1747-1567.2007.00182.x, ISSN 0732-8818.
Sun, Y., Luo, Y., Wang, X., 2012. Micro energy director array in ultrasonic precise bonding for thermoplastic micro assembly. J. Mater. Process. Technol. 212 (6), 1331–1337, http://dx.doi.org/10.1016/j.jmatprotec.2012.01.013, ISSN 0924-0136.

Truckenmuller, R., Ahrens, R., Cheng, Y., Fischer, G., Saile, V., 2006. An ultrasonic welding based process for building up a new class of inert fluidic microsensors and actuators from polymers. Sens. Actuators: A Phys. 385 (1), http://dx.doi.org/10.1016/j.sna.2006.04.040, ISSN 0924-4247.

Wineman, A.S., Rajagopal, K.R., 2000. Mechanical Response of Polymers: An Introduction. Cambridge University Press, Cambridge, ISBN 0-521-64337-6 0-521-64409-7.

Zhang, Z.B., Wang, X.D., Luo, Y., He, S.Q., Wang, L.D., 2010a. Thermal assisted ultrasonic bonding method for poly(methyl methacrylate) (PMMA) microfluidic devices. Talanta 81 (4), 1331–1338.

Zhang, Z., Luo, Y., Wang, X., Zheng, Y., Zhang, Y., Wang, L., 2010b. A low temperature ultrasonic bonding method for PMMA microfluidic chips. Microsyst. Technol. 533 (4), ISSN 0946-7076.